WeeklyNote

2019.11.10

張慕琪

Theoretical and Applied Climatology (2019) 137:1729–1746
https://doi.org/10.1007/s00704-018-2686-z

ORIGINAL PAPER

ANN-based statistical downscaling of climatic parameters using decision tree predictor screening method

Vahid Nourani [1,2] · Zahra Razzaghzadeh [1] · Aida Hosseini Baghanam [1] · Amir Molajou [3]

Received: 13 September 2018 / Accepted: 16 October 2018 / Published online: 12 November 2018

Introduction

计算成本低、简便

降尺度

统计降尺度　　建立GCM和所需尺度内水文气候变量间的经验统计关系

动力降尺度　　基于物理方程以达到同样目的

Method

15个GCMs(CMIP3, CMIP5)；

Tabriz station(Tabriz airport) for the period of 1951-2016；

时间： 1951-2000(calibration)、2020-2060(validation)

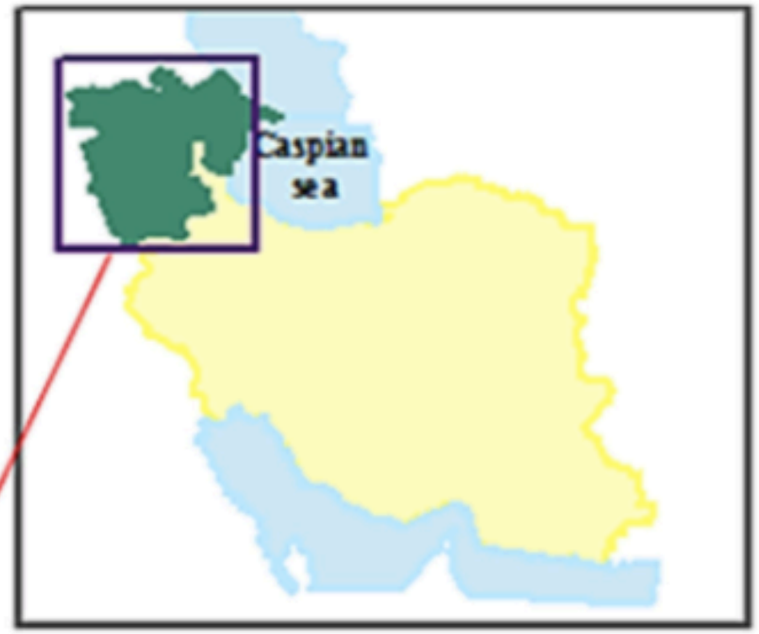

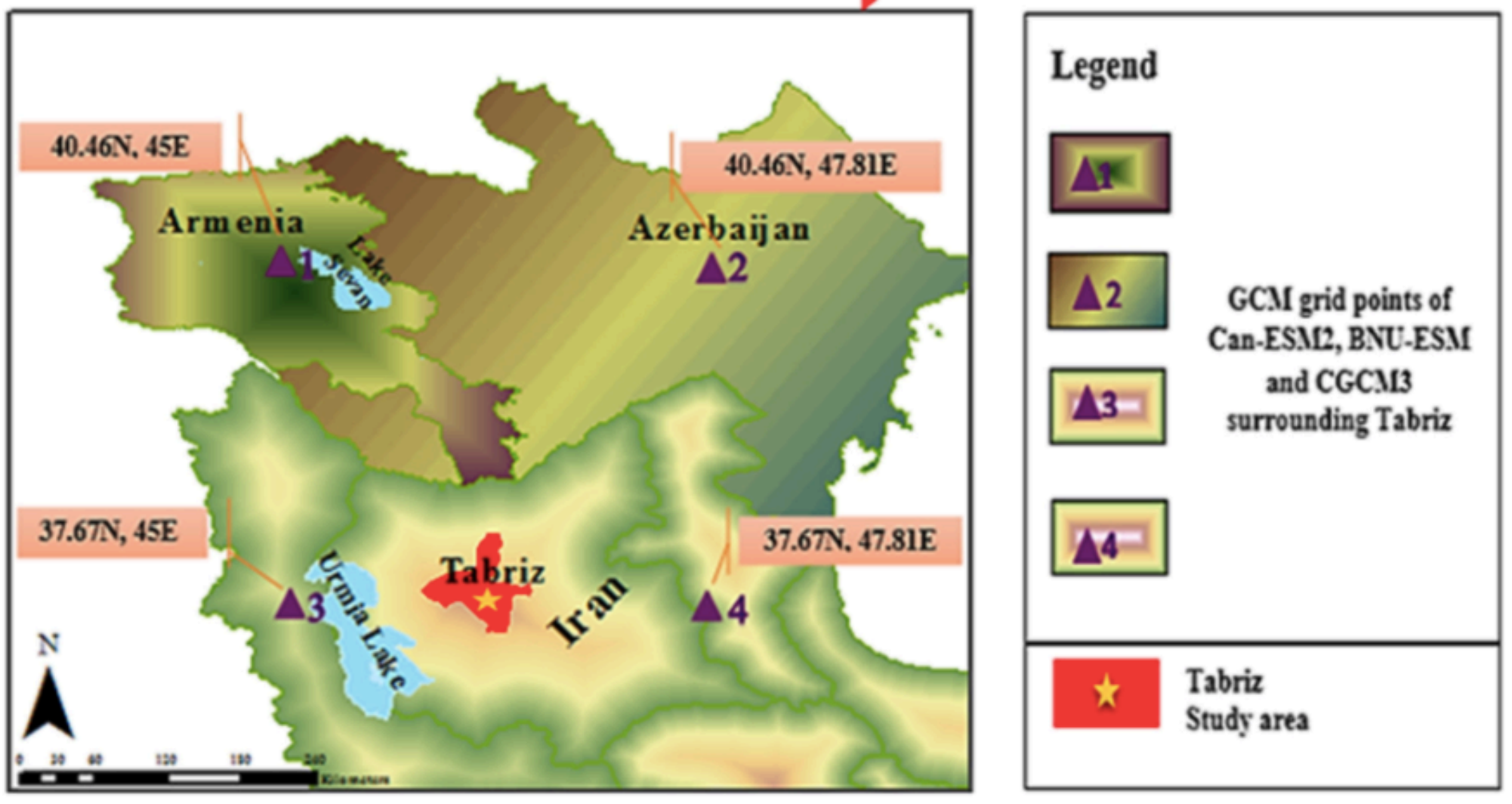

Fig. 1 Geographical location of the study area

Method

Table 1 The considered GCM models in order to select the suitable GCM for downscaling

	Model	Resolutions (lat° × lon°)	Country	Research center
(CMIP3) models	CSIRO-MK3.0	1.9° × 1.9°	Australia	Commonwealth Scientific and Industrial Research Organization
	CGCM3(T47)	3.8° × 3.8°	Canada	Canadian Center for Climate Modeling and Analysis
	CGCM3(T63)	2.8° × 2.8°	Canada	Canadian Center for Climate Modeling and Analysis
	FGOALS-g1.0	2.8° × 3°	China	Institute of Atmospheric Physics
	Had-CM3	3.8° × 2.5°	UK	UK Meteorological Office
	GFDL-CM2.1	2.5° × 2°	USA	Geophysical Fluid Dynamics Laboratory
	NCAR-CCSM3	1.4° × 1.4°	USA	National Centre for Atmospheric Research
(CMIP5) model	ACCESS1.0	1.2° × 1.9°	Australia	Commonwealth Scientific and Industrial Research Organization
	CSIRO-MK3.6.0	1.9° × 1.9°	Australia	Commonwealth Scientific and Industrial Research Organization
	Can-ESM2	2.8° × 2.8°	Canada	Canadian Centre for Climate Modeling and Analysis
	BNU-ESM	2.8° × 2.8°	China	Beijing Normal University
	FIO-ESM	2.8° × 2.8°	China	The First Institute of Oceanography, SOA
	IPSL-CM5B-LR	1.9° × 3.7°	France	Institute Pierre Simon Laplace
	HadGEM2-AO	1.2° × 1.9°	Korea	National Institute of Meteorological Research
	GISS--E2-R-CC	2° × 2.5°	USA	NASA/GISS (Goddard Institute for Space Studies)

Method

Table 2 List of the applied predictors in the current study

Predictors	Predictors description	Height
pr	Precipitation	Surface
prc	Convective precipitation	Surface
prw	Atmosphere water vapor content	Surface
hfls	Surface upward latent heat flux	Surface
evspsbl	Water evaporation	Surface
rsds	Downwelling shortwave flux	Surface
rtmt	Net downward radiative flux at top of atmosphere	Surface
rlus	Upwelling longwave radiation	Surface
rsdt	Toa_incoming shortwave flux	Surface
rlut	Toa outgoing longwave flux	Surface
sund	Sunshine hours	Surface
rsut	Toa outgoing shortwave flux	Surface
ts	Sea surface temperature	Surface
tauu	Downward eastward wind stress	Surface
tauv	Downward northward wind stress	Surface
tasmin	Minimum air temperature	Surface
tasmax	Maximum air temperature	Surface
ps	Surface air pressure	Surface
psl	Sea level pressure	Surface
wap	Lagrangian tendency of air pressure	Surface
clivi	Atmosphere mass content of cloud ice	Surface
clt	Cloud area fraction	Surface
clwvi	Cloud condensed water content	Surface
mslp	Monthly mean sea level pressure	Surface
snc	Snow area fraction	Surface
sci	Shallow convection time fraction	Near surface
hurs	Relative_humidity	Near surface
vas	Meridional wind speed	Near surface
uas	Zonal wind speed	Near surface
huss	Specific humidity	Near surface
tas	Air temperature	Near surface
sfcwind max	Daily max near surface wind speed	Near surface
sfcwind	Wind speed	Near surface
wap	Lagrangian tendency of air pressure	Various pressure levels[(a)]
ta	Air temperature	Various pressure levels[(a)]
zg	Geopotential height	Various pressure levels[(a)]
ua	Zonal wind	Various pressure levels[(a)]
va	Meridional wind	Various pressure levels[(a)]
hur	Relative humidity	Various pressure levels[(a)]
hus	Specific humidity	Various pressure levels[(a)]

[(a)] 10 hpa, 20 hpa, 30 hpa, 50 hpa, 70 hpa, 100 hpa, 200 hpa,300 hpa, 400 hpa, 500 hpa, 600 hpa, 700 hpa, 850 hpa, 1000 hpa

Method

1951-2016月平均降水和温度

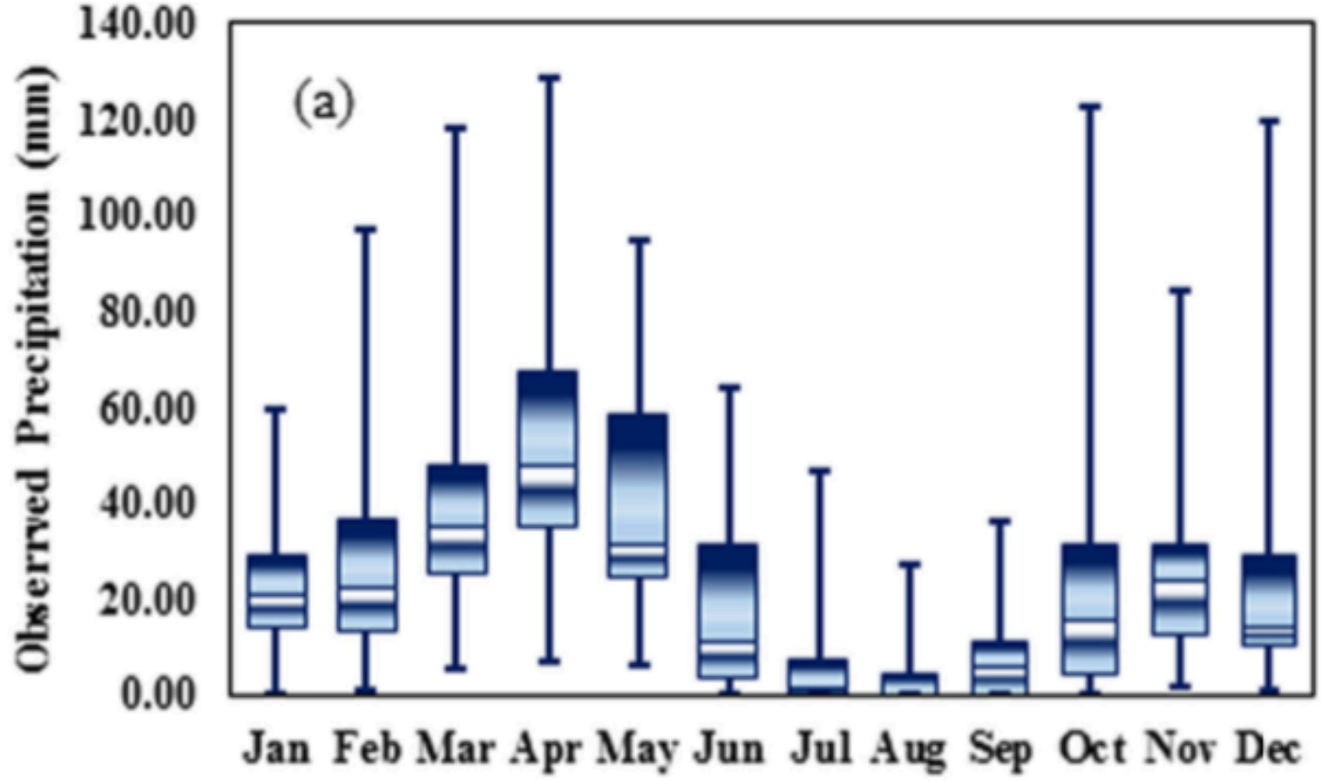

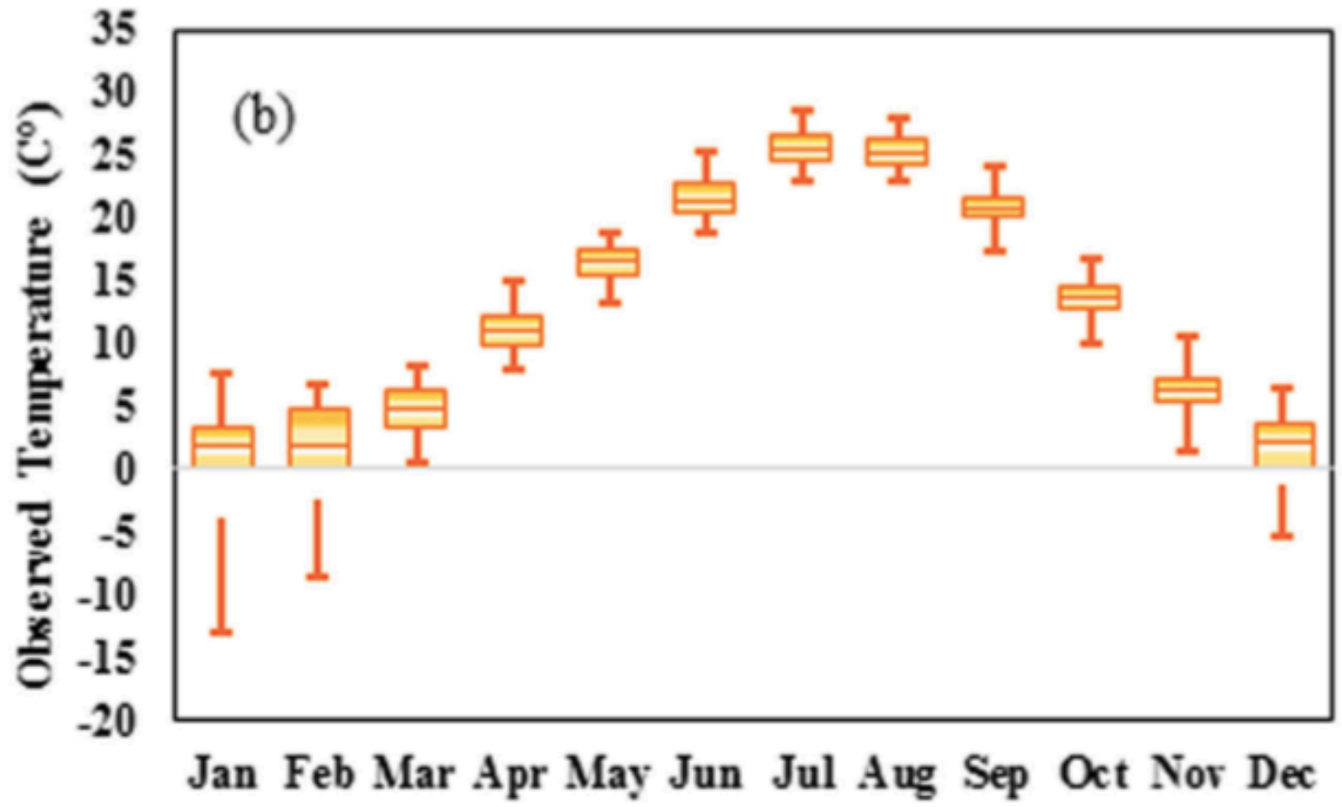

Method

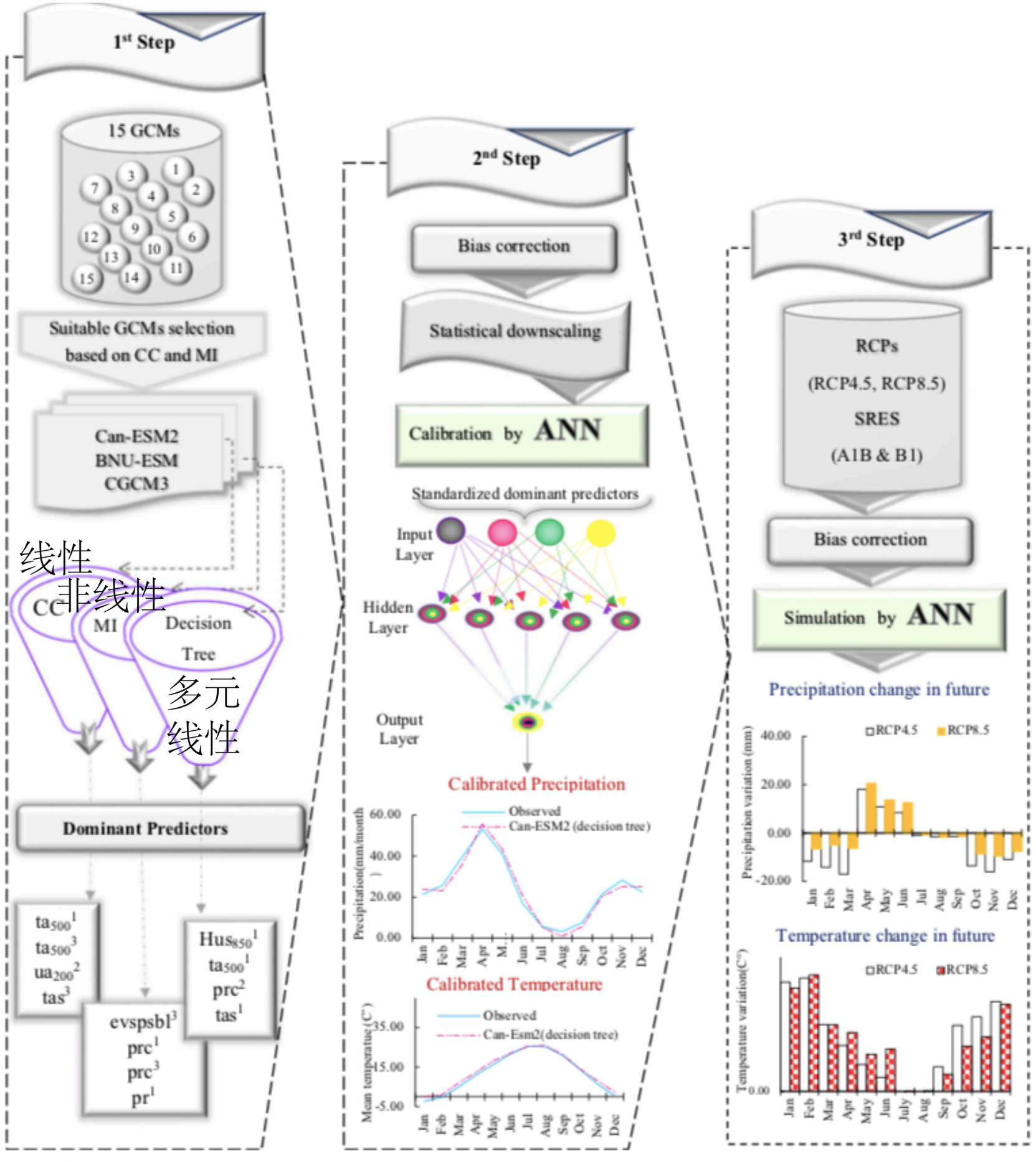

Fig. 3 Schematic figure of the proposed methodology. (It is noted that dominant predictors in this figure belong to Can-ESM2 model as an example)

Results

Table 3 Appropriate GCM selecting according to CC and MI measures

		Precipitation		Temperature	
	Model	CC*	MI*	CC*	MI*
CMIP5	ACCESS1.0	0.41	0.51	0.55	0.71
	CSIRO-MK3.6.0	0.39	0.48	0.51	0.70
	Can-ESM2	0.62	0.86	0.75	0.98
	BNU-ESM	0.58	0.79	0.70	0.91
	FIO-ESM	0.26	0.32	0.47	0.66
	IPSL-CM5B-LR	0.43	0.24	0.57	0.74
	HadGEM2-AO	0.37	0.43	0.50	0.69
	GISS--E2-R-CC	0.33	0.41	0.50	0.67
CMIP3	CSIRO-MK3.0	0.25	0.34	045	0.65
	CGCM3(T47)	0.49	0.70	0.60	0.82
	CGCM3(T63)	0.16	0.21	0.37	0.59
	FGOALS-g1.0	0.19	0.28	0.39	0.60
	Had-CM3	0.21	0.30	0.40	0.62
	GFDL-CM2.1	0.30	0.39	0.47	0.65
	NCAR-CCSM3	0.32	0.40	0.51	0.67

*The result of grid point with high relevancy with observed data

Results

Table 4 Selection of the dominant predictors according to three screening methods

Model	Feature extraction method	Dominant predictors for precipitation[(i)]	Dominant predictors for temperature[(i)]
Can-ESM2	CC	Pr(1),Prc(1),Prc(3),evspsbl(3)	ta(200)(3),ta(200)(4),ta(500)(1),ta(500)(3)
	MI	ta(500)(1),ta(500)(3),tas(3),ua(200)(2)	zg(500)(1),ua(500)(3),zg(500)(4),hurs(3)
	Decision tree	Prc(2),hus(850)(2),tas(1),ta(500)(1)	zg(200)(2),tas(1),zg(200)(1),hur(200)(2)
BNU-ESM	CC	prw(2),evspsbl(3),huss(1),prc(1)	ta(500)(1),ta(500)(2),ta(500)(3),ta(500)(4)
	MI	ua(850)(1),ta(850)(3),ua(200)(3),ta(850)(1)	hur(850)(1),ua(850)(3),ua(850)(3),zg(200)(3)
	Decision tree	ta(200)(2),ts(1),ta(1000)(1),pr(3)	zg(500)(2),zg(200)(1),ta(200)(2),evspsbl(1)
CGCM3	CC	Pr(1), evspsbl (3),hurs(2),pr(2)	tas(1),tas(2),tas(3),tas(4)
	MI	tas(2),tas(1),ts(1),ua(500)(2(	zg(200)(2),ua(200)(1),psl(4),huss(2)
	Decision tree	Pr(3),Pr(1),ts(1), tas(2)	tas(1),zg((500)(3),psl(3),huss(3)

[(i)] The number of GCMs grid points based on Fig. 1 ($i = 1, 2, 3, 4$)

Results

Table 5 The results of precipitation downscaling by ANN and MLR models using dominant inputs extracted by CC, MI, and decision tree

Feature extraction method	Inputs	GCM	Downscaling model	NSE training	NSE testing	RMSE* training	RMSE* testing
CC	Pr(1),Prc(1),Prc(3),evspsbl(3)	Can-ESM2	ANN	0.56	0.53	0.52	0.53
CC	Pr(1),Prc(1),Prc(3),evspsbl(3)	Can-ESM2	MLR	0.47	0.44	0.57	0.60
MI	ta(500)(1),ta(500)(3),tas(3),ua(200)(2)	Can-ESM2	ANN	0.69	0.65	0.34	0.37
MI	ta(500)(1),ta(500)(3),tas(3),ua(200)(2)	Can-ESM2	MLR	0.40	0.36	0.64	0.68
Decision tree	Prc(2),hus(850)(2),tas(1),ta(500)(1)	Can-ESM2	ANN	0.85	0.83	0.19	0.23
Decision tree	Prc(2),hus(850)(2),tas(1),ta(500)(1)	Can-ESM2	MLR	0.61	0.58	0.39	0.47
CC	prw(2),evspsbl(3),huss(1),prc(1)	BNU-ESM	ANN	0.52	0.49	0.55	0.57
CC	prw(2),evspsbl(3),huss(1),prc(1)	BNU-ESM	MLR	0.44	0.40	0.62	0.66
MI	ua(850)(1),ta(850)(3),ua(200)(3),ta(850)(1)	BNU-ESM	ANN	0.65	0.61	0.35	0.41
MI	ua(850)(1),ta(850)(3),ua(200)(3),ta(850)(1)	BNU-ESM	MLR	0.40	0.37	0.61	0.69
Decision tree	ta(200)(2),ts(1),ta(1000)(1),pr(3)	BNU-ESM	ANN	0.79	0.77	0.25	0.30
Decision tree	ta(200)(2),ts(1),ta(1000)(1),pr(3)	BNU-ESM	MLR	0.55	0.53	0.50	0.54
CC	Pr(1), evspsbl (3),hurs(2),pr(2)	CGCM3	ANN	0.41	0.37	0.67	0.69
CC	Pr(1), evspsbl (3),hurs(2),pr(2)	CGCM3	MLR	0.34	0.32	0.72	0.73
MI	tas(2),tas(1),ts(1),ua(500)(2(	CGCM3	ANN	0.51	0.46	0.55	0.59
MI	tas(2),tas(1),ts(1),ua(500)(2((	CGCM3	MLR	0.32	0.29	0.75	0.78
Decision tree	Pr(3),Pr(1),ts(1), tas(2)	CGCM3	ANN	0.62	0.59	0.39	0.45
Decision tree	Pr(3),Pr(1),ts(1), tas(2)	CGCM3	MLR	0.45	0.41	0.63	0.65

*indicates normalized RMSE values

Results

Table 6 The results of temperature downscaling by ANN and MLR models using dominant inputs extracted by CC, MI, and decision tree

Feature extraction method	Inputs	GCM	Downscaling model	NSE calibration	NSE validation	RMSE* calibration	RMSE* validation
CC	ta(200)(3),ta(200)(4),ta(500)(1),ta(500)(3)	Can-ESM2	ANN	0.61	0.57	0.30	0.37
CC	ta(200)(3),ta(200)(4),ta(500)(1),ta(500)(3)	Can-ESM2	MLR	0.67	0.61	0.27	0.31
MI	zg(500)(1),ua(500)(3),zg(500)(4),hurs(3)	Can-ESM2	ANN	0.75	0.71	0.15	0.20
MI	zg(500)(1),ua(500)(3),zg(500)(4),hurs(3)	Can-ESM2	MLR	0.59	0.53	0.35	0.43
Decision tree	zg(200)(2),tas(1),zg(200)(1),hur(200)(2)	Can-ESM2	ANN	0.94	0.91	0.06	0.08
Decision tree	zg(200)(2),tas(1),zg(200)(1),hur(200)(2)	Can-ESM2	MLR	0.75	0.69	0.16	0.22
CC	ta(500)(1),ta(500)(2),ta(500)(3),ta(500)(4)	BNU-ESM	ANN	0.59	0.56	0.33	0.39
CC	ta(500)(1),ta(500)(2),ta(500)(3),ta(500)(4)	BNU-ESM	MLR	0.66	0.59	0.27	0.33
MI	hur(850)(1),ua(850)(3),ua(850)(3),zg(200)(3)	BNU-ESM	ANN	0.72	0.71	0.20	0.23
MI	hur(850)(1),ua(850)(3),ua(850)(3),zg(200)(3)	BNU-ESM	MLR	0.57	0.50	0.38	0.45
Decision tree	zg(500)(2),zg(200)(1),ta(200)(2),evspsbl(1)	BNU-ESM	ANN	0.95	0.89	0.06	0.11
Decision tree	zg(500)(2),zg(200)(1),ta(200)(2),evspsbl(1)	BNU-ESM	MLR	0.75	0.67	0.15	0.24
CC	tas(1),tas(2),tas(3),tas(4)	CGCM3	ANN	0.49	0.45	0.47	0.50
CC	tas(1),tas(2),tas(3),tas(4)	CGCM3	MLR	0.54	0.51	0.38	0.47
MI	zg(200)(2),ua(200)(1),psl(4),huss(2)	CGCM3	ANN	0.58	0.56	0.35	0.38
MI	zg(200)(2),ua(200)(1),psl(4),huss(2)	CGCM3	MLR	0.49	0.44	0.48	0.52
Decision tree	tas(1),zg((500)(3),psl(3),huss(3)	CGCM3	ANN	0.79	0.77	0.15	0.16
Decision tree	tas(1),zg((500)(3),psl(3),huss(3)	CGCM3	MLR	0.63	0.59	0.28	0.32

*indicates normalized RMSE values

Results

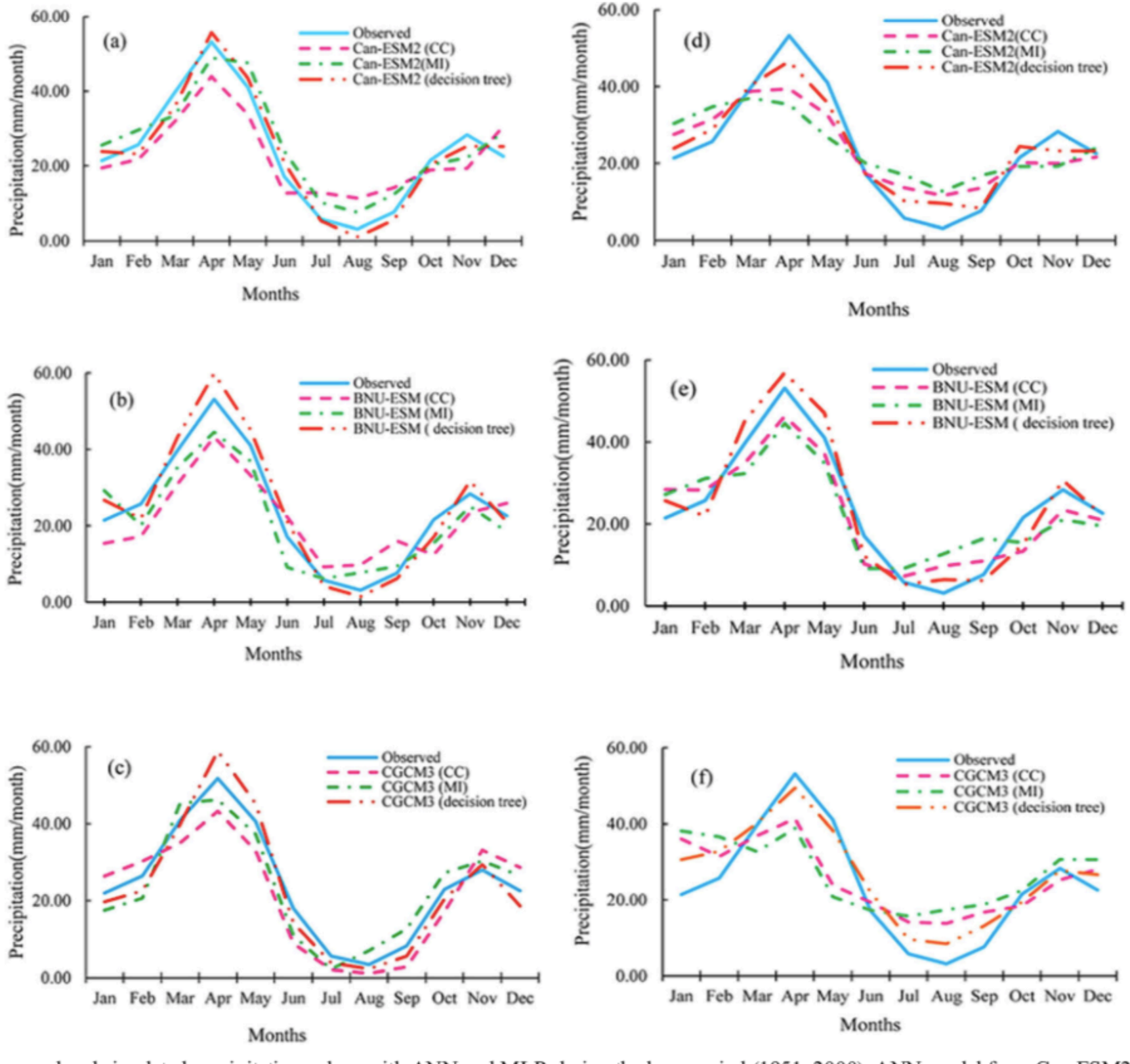

Fig. 5 Observed and simulated precipitation values with ANN and MLR during the base period (1951–2000). ANN model for **a** Can-ESM2, **b** BNU-ESM, and **c** CGCM3. MLR model for **d** Can-ESM2, **e** BNU-ESM, and **f** CGCM3

Results

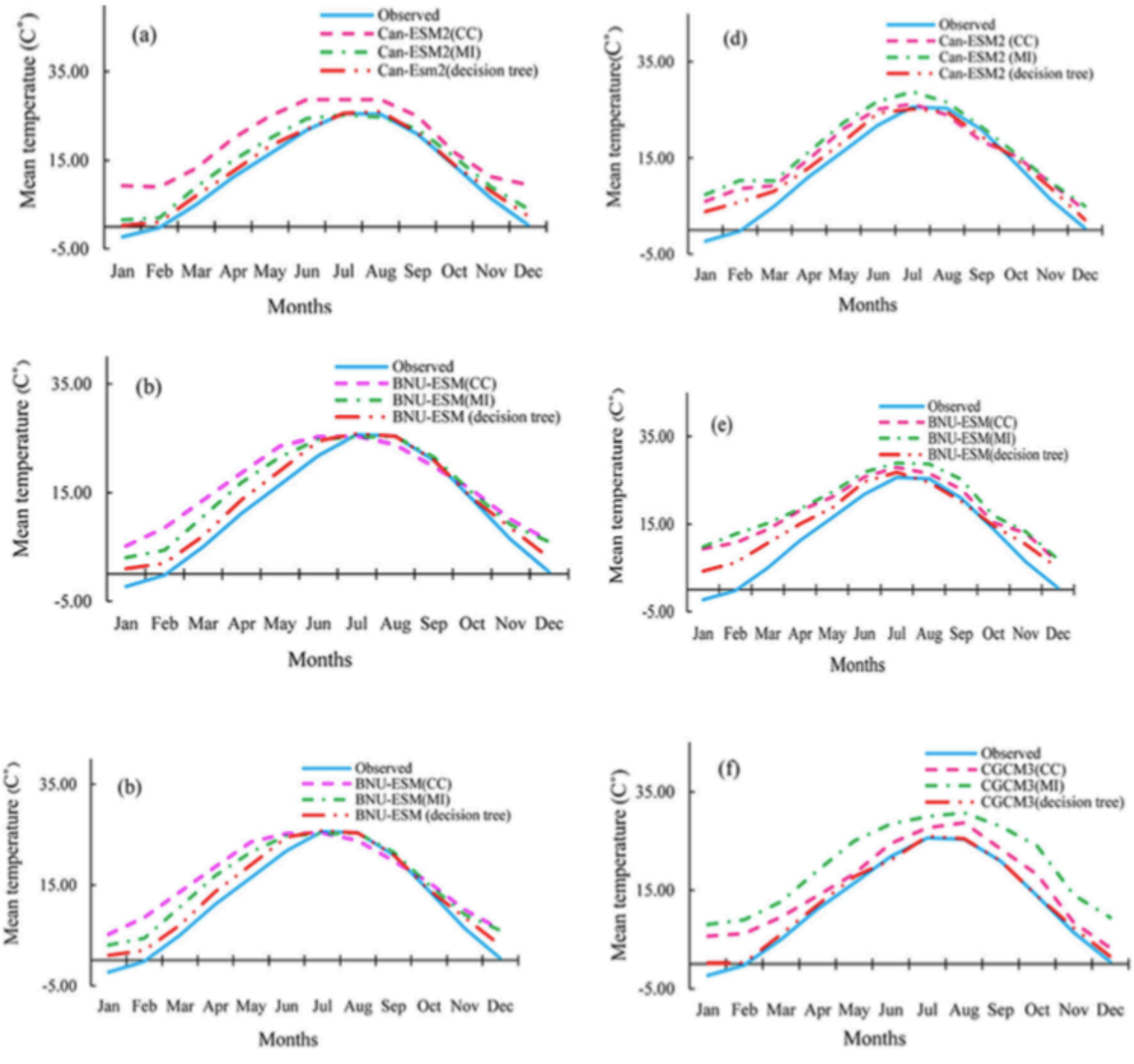

Fig. 6 Observed and simulated temperature values with ANN and MLR during the base period (1951–2000). Simulated temperature with ANN respectively for three GCMs, **a** Can-ESM2, **b** BNU-ESM, and **c** CGCM3. Simulated temperature with MLR model respectively for three GCMs, **d** Can-ESM2, **e** BNU-ESM, and **f** CGCM3

Results

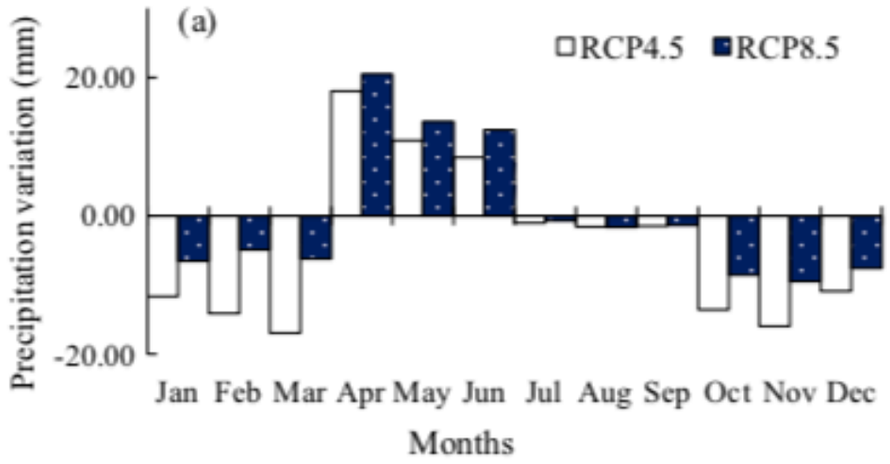

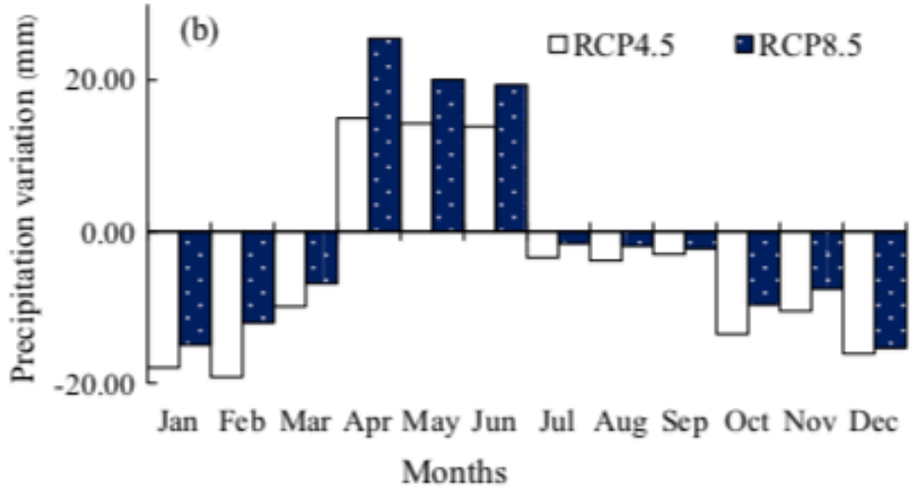

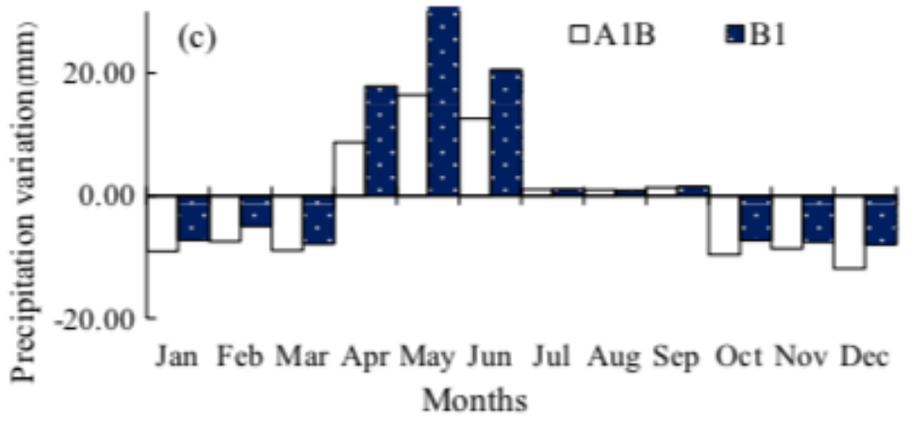

Fig. 7 Monthly precipitation variation according to projected and baseline periods for **a** Can-ESM2, **b** BNU-ESM, and **c** CGCM3 models

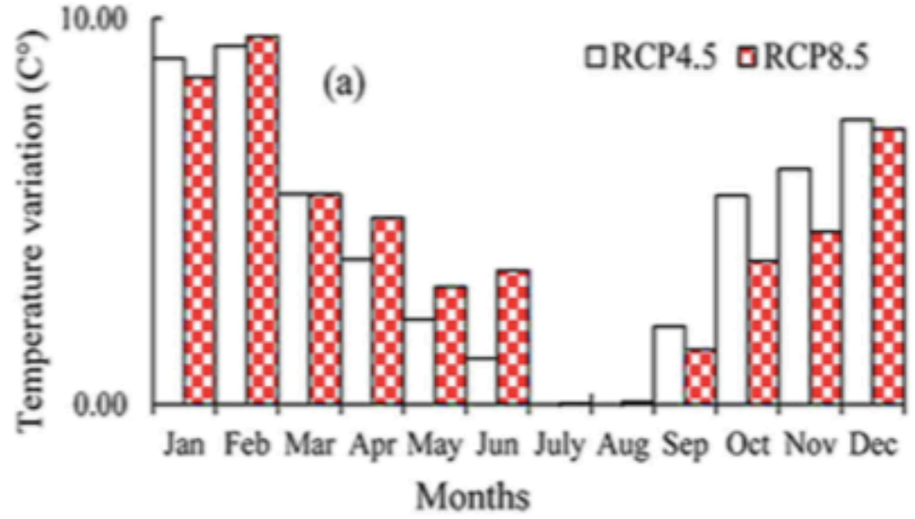

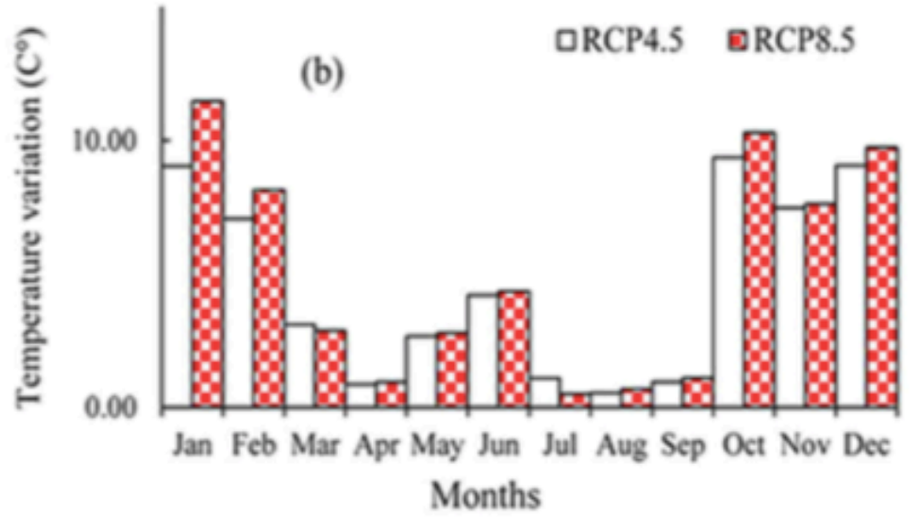

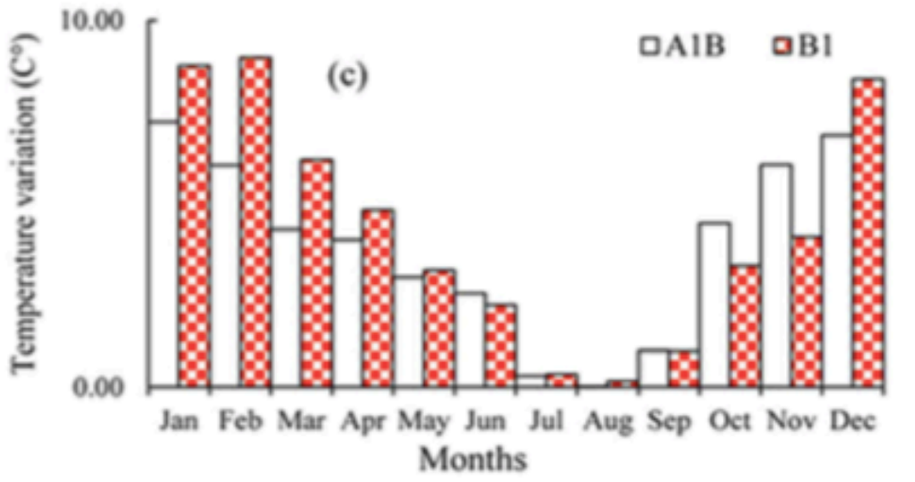

Fig. 8 Monthly temperature variation according to projected and baseline periods for Can-ESM2, **b** BNU-ESM, **c** CGCM3 models

Results

Fig. 9 The change percentage of annual observed and simulated **a** precipitation and **b** temperature

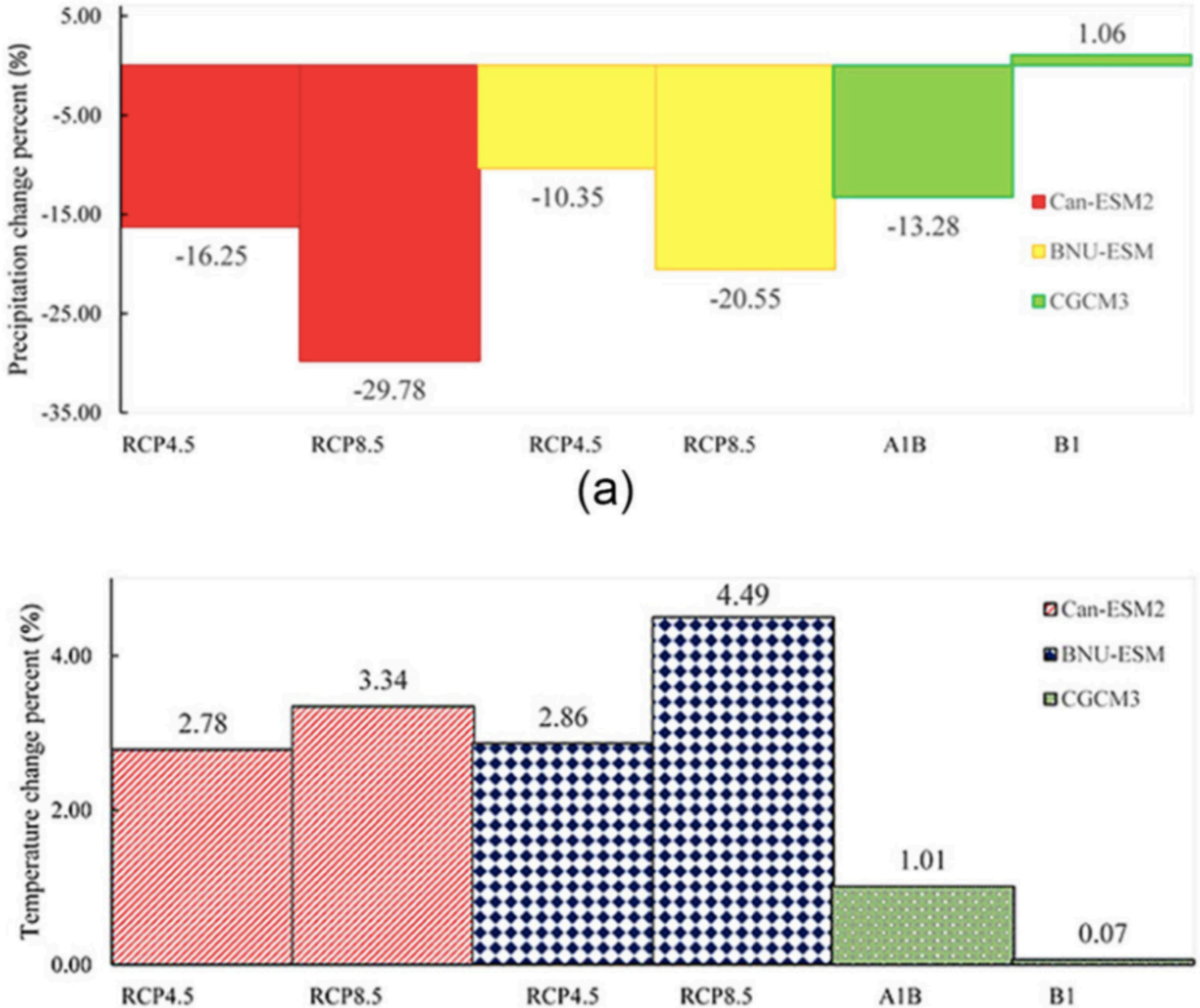

Conclusions

1. 使用非线性的决策树方法且基于ANN方法的降尺度模型比使用CC和MI（线性方法）更加准确；
2. 使用非线性的决策树方法且基于ANN方法的降尺度模型在降水和温度两个变量上比MLR方法准确率提高了31%和25%；
3. 未来的降水和温度既有增加的时候也有减少的时候。这暗示了全球变暖正在发生，全球温度上升、海平面上升都会使降水的特征和总量发生变化；
4. 本文认为未来降水将减少10.35-29.78%，而温度将上升0.06-2.49%。

谢谢